Calculation, Evaluation and Application of Long-term, Global Radiative Flux Datasets at ISCCP: Past and Present

By Yuanchong Zhang[1, 4], William B. Rossow[2], Andrew A. Lacis[3] and Valdar Oinas[4]

[1]Department of Applied Physics and Applied Mathematics, Columbia University and NASA Goddard Institute for Space Studies, New York, NY, USA, (Retired)
[2]CREST at the City College of New York, NY, USA, (Retired)
[3]NASA Goddard Institute for space Studies, New York, NY, USA
[4]SciSpace, LLC, New York, NY, USA

Yuanchong Zhang (PhD in Geophysics from Columbia University, 1990) is a retired Research Scientist from Columbia University and NASA Goddard Institute for Space Studies. His research activities/interests include calculating global, 3-hourly and long-term radiative flux profiles that have resulted in the ISCCP FC, FD and FH products, validating flux results, studying global radiation/energy budgets, general circulation/energy transports for the whole atmosphere-earth system and its separate atmospheric and oceanic components, and cloud-radiation interactions as well as studying Earth Tides, Seismology, etc.

William B. Rossow (PhD in Astronomy from Cornell University, 1976) is Emeritus Distinguished Professor of Remote Sensing at The City College of New York and former Senior Research Scientist at NASA Goddard Institute for Space Studies. His research covered cloud physics and dynamics, atmospheric general circulations, atmospheric radiative transfer and radiation budgets, satellite remote sensing of all components of Earth's climate system, and advanced analysis of climate and climate feedbacks. He was the Head of the Global Processing Center for the World Climate Research Program's International Satellite Cloud Climatology Project (ISCCP) from 1982 to 2017.

Andrew A. Lacis (PhD in Physics from University of Iowa, 1970) is a Senior Research Scientist at the NASA Goddard Institute for Space Studies (GISS) in New York City. He has been a member of the GISS climate modeling group since the mid-1970s. His area of expertise is development of fast and accurate radiative transfer techniques to model solar and thermal radiation with applications to the study of global climate change and the remote sensing of planetary atmospheres. He is the principal architect of the radiation modeling methodology that is used in the GISS climate GCM.

Valdar Oinas (PhD in Astronomy from California Institute of Technology, 1971) is a senior research scientist at NASA Goddard Institute for Space Studies (GISS) in New York. Now fully retired from teaching physics at the CUNY Queensborough College in New York, Dr. Oinas has also been a member of the GISS climate modeling group since the mid-1970s. His chief area of expertise is the development of fast and accurate radiative transfer techniques to model solar and thermal radiation in the study of global climate change with applications also to remote sensing. He has been a key developer of the GISS GCM radiation modeling methodology.

Introduction

It should never be overemphasized that the tempo-spatial variations of all the forms of energy in the atmosphere and at the surface are vitally important to any branch of earth sciences as well as human lives.

Among all the forms of energy exchanges, radiative fluxes play a fundamental role as it is virtually the only way for energy exchange between the earth-atmosphere system and outer space and it is the primary driving force in the general circulation of the whole atmosphere-ocean system.

There are three main inference methods for estimating global radiative fluxes at the top of atmosphere (TOA), surface and in the atmosphere, namely, (1) regression methods based on satellite observations (see, e.g., Cess and Vulis, 1989) often with assistance of some radiation model, (2) so-called 'Look-Up Table (LUT) approaches' or 'matching' methods that match radiative transfer computations and satellite observations to infer the desired radiative fluxes at TOA and at the surface under various scenarios (see, e.g., Ma and Pinker, 2012) and (3) detailed flux calculation methods that use observation-based physical parameters as realistic as possible for all the associated atmospheric and surface properties as inputs to a detailed, relatively accurate and efficient radiative transfer model to calculate fluxes. This third method is probably the most comprehensive and more physically meaningful method that we have employed since the beginning of the ISCCP flux-calculation project. The project was pioneered by Rossow and Lacis (1990), but the production of an actual global flux product had to wait for a global, comprehensive cloud data product to appear, which is the first generation of the International Satellite Cloud Climatology Project (ISCCP) datasets, the C-series product, or ISCCP-C (Schiffer and Rossow, 1983; Rossow and Schiffer, 1991). This is because all of the global cloud climatologies prior to the ISCCP-C usually report on cloud amount only and do not contain sufficient information on cloud-top temperature (or altitude) and/or on the optical properties of clouds required by climate modelers to calculate the first-order effects of clouds on the earth's radiation budget or the climate feedbacks produced by cloud variations (Stockholm, 1975). The ISCCP-C product for the first time made it possible for us to use the detailed radiation model of the NASA Goddard Institute for Space Studies (GISS) GCM Model II (Hansen et al. 1983) to calculate global, satellite-observation-based radiative fluxes at TOA and surface, which is our first-generation global flux product, the ISCCP-FC (Zhang et al., 1995), where the acronym FC means Flux calculated (mainly) using C data (ISCCP-C, or C-series, and similarly for FD and FH for the second and third generation flux products as described below).

In the following years, ISCCP has developed two more generations of its products, D-series (Rossow and Schiffer, 1999) and the current H-series products (Young et al., 2018). The ISCCP-D product reported separate cloud properties for liquid and ice forms of low and middle-level clouds along with other many important improvements (Rossow and Schiffer, 1999) and, as the third generation product, the ISCCP-H has been more advanced. Instead of using every-30-km-sampled B3 for ISCCP-D, ISCCP-H uses 10-km-sampled B1. There are also other refinements in radiance quality control (QC), calibration, cloud detection (especially high, thin and polar clouds), cloud and surface property retrievals with more modern and more homogeneous ancillary datasets, e.g., more accurate surface type and topography, snow/ice datasets, reprocessed ozone data, etc. The cloud and surface retrievals are now based on more realistic atmospheric properties, with MACv1 aerosols (Kinne, 2013) included so the uncertainties are reduced as all the ancillary datasets have been improved. The temperature and humidity profiles with increased vertical resolution have been statistically adjusted to have diurnal variation wherever suitable. The new ISCCP H-series has also increased sub-data product categories (e.g., five for L3) with a new globally gridded pixel-level (L2) data.

Accordingly, we have developed and produced the next two generations of radiative profile flux products, namely, the ISCCP-FD (Zhang et al., 2004) and the current ISCCP-FH, which are based on improved NASA GISS radiation models of the GCM ModelD, or SI2000 (Hansen et al. 2002) and ModelE (Schmidt et al. 2006), respectively. All the three generations of the flux products are global, with the same temporal and spatial resolution as their corresponding ISCCP products. Moreover, FD and FH have added fluxes at three levels in the atmosphere (between TOA and the surface) as a cloud vertical structure (CVS) model is introduced to construct realistic vertical cloud layers instead of using single, fixed 100-hPa-thick cloud layers as in ISCCP-FC. The temporal coverage is the Earth Radiation Budget Experiment (ERBE) period for ISCCP-FC while ISCCP-FD covered July 1983 to December 2009. The ISCCP-FH products now cover the period from July 1983 to

June 2017 (34 years) and will be extended whenever the ISCCP-H is completed. Both the ISCCP-FH (version 0.0) and ISCCP-FD products (version 0.0 except 2001 of v. 0.01) are publically available online at:

https://isccp.giss.nasa.gov/projects/flux.html

The ISCCP-FH product may also become publically available at NOAA National Centers for Environmental Information (NCEI).

The core of all the NASA GISS radiation models is the correlated K-distribution method as described in Hansen et al. (1983) for GCM Models I and II. Since then, the spectral resolution has been increased by increasing the number of the noncontiguous correlated spectral resolution intervals, K, to obtain higher accuracy from 12 and 25 to the current 16 and 33 for shortwave (SW) and longwave (LW), respectively, paralleling the evolution of the GISS GCM models I and II to SI2000 or ModelD (Hansen et al. 2002), and to ModelE (Schmidt et al. 2006). The radiation part of the GCM Model II, code-named RadII, was used for the ISCCP-FC production while ModelD's radiation part, code-named RadD, for the ISCCP-FD flux profile product (Zhang et al., 2004). Based on the radiation part of the GISS GCM ModelE (of 2011), code-named RadE, we have developed the current radiation calculation code, RadH. RadE (and therefore RadH) has an accuracy of 1 W/m^2 for cooling rates (in degree/day) throughout the troposphere and most of the stratosphere as compared with line-by-line calculations (Lacis and Oinas, 1991) for LW, and is close to 1% for SW for RadE/RadH now. The major advanced features of RadH include: (1) reformulation of the SW line absorption for H2O, O2, CO2, CH4, N2O, etc. using the latest HITRAN2012 atlas (Rothman et al., 2013) with additional weak-SW-absorption values for H2O, O2 and CO2, (2) corrections of some H2O deficiencies, especially for large water vapor amounts (see, e.g., DeAngelis, et al., 2015), so it is improved in terms of accuracy, spectral coverage, additional absorption phenomena, and validity, (3) use of a new global aerosol data MAC-v2, based on AeroCom's advances (Kinne, 2013), (4) improved LW modeling of the H2O continua, CFC absorption cross-sections, SO2 line absorption, CH4 and N2O overlap treatment and polar region (conditions) profile calculations, (5) improved vertical cloud layer construction using the Vertical Cloud Layer Configuration (VCLC) algorithm that uses 5-year CloudSAT-CLIPSO climatology (Stephens et al., 2002), and (6) new TSI (total solar irradiance) is introduced, which is a self-consistent daily time series based on SORCE V-15, Davos WRC composite and RMIB (from Dr. Shashi Gupta). The RadH is equivalent to the radiation code of the current NASA GISS ModelE2.1 (Kelley et al., 2020).

All the three generations of the radiation models (RadII, RadD and RadH) that we have adopted for ISCCP-FC, FD and FH production have the following good features: (1) the atmosphere from the surface to the top of the atmosphere (TOA) can be physically divided into any number of layers at any pressure level so that, e.g., physical cloud layers can be positioned precisely at any altitude and interleaved with clear air layers just like in the real world, (2) all the input parameters are physical quantities that can be as realistic as possible and naturally and realistically variable in each cloud or air layer as well as at the surface (for example, each cloud layer has its own top and base temperatures and pressures, optical thickness, and microphysical model specified by the phase, particle shape, effective particle size and size distribution variance. All air/cloud layers can also have their own aerosol mixtures with different optical properties, i.e., all the constituents and their physical properties in the model can be specified vertically independently), (3) the corresponding output fluxes were calculated for all the specified interfaces of the air/cloud layers, including TOA and the surface, for all the downwelling and upwelling broadband shortwave (SW of 0.2 to 5.0 μm) and longwave (LW of 5.0 to 200 μm) component fluxes (with additional downward SW direct and diffuse fluxes at surface but for ISCCP-FH only) for all-sky, clear-sky and overcast scenes, (4) the model is detailed and complete (i.e., not for a "bulk" atmosphere, etc.) and is physically self-consistent at all wavelengths, i.e., SW and LW are all treated using correlated k-distribution (CKD) method, atmospheric and surface properties are from consistent data sources, so it can be used to diagnose/determine the radiative heating/cooling effects of any specific physical parameter(s)

and/or structure(s) of the atmosphere, clouds and surface in a consistent way (the self-consistency may help reduce some flux errors), (5) with improvements of the accuracy and knowledge of all input physical quantities, as well as the radiative transfer theory itself, the model can be relatively easily updated to incorporate any newly available information (for example, when ice cloud detection became feasible and better information about their properties became available in ISCCP-D data that had new, separated ice and liquid clouds, RadD was able to use this information to produce ISCCP-FD flux profile product with the better cloud information for both the ice and liquid clouds).

Various methods have been used to validate/evaluate our flux products (ISCCP-FC, FD and FH) mainly using observations of ERBE and the Clouds and the Earth's Radiant Energy System (CERES, Wielicki et al., 1996) at TOA and the Global Energy Balance Archive (GEBA, Ohmura and Gilgen, 1991) and the Baseline Surface Radiation Network (BSRN, Ohmura, 1998) at surface and other flux products [see Rossow and Zhang (1995) and Zhang et al., (2004), respectively, for the validation of the ISCCP-FC and FD, and see accompanying slides for ISCCP-FH]. Based on our previous validation and for regional, monthly mean fluxes, the ISCCP-FC has overall uncertainties of 10 – 15 W/m^2 at TOA and 20 – 25 W/m^2 at surface while the ISCCP-FD has been improved to smaller 5 – 10 W/m^2 at TOA and 10 – 15 W/m^2 at surface (The latter probably underestimated, see slides 2 and 18 – 19). The preliminary uncertainties of the ISCCP-FH are overall slightly better than FD (especially for atmospheric SW absorption and surface fluxes) with FH's increased spatial resolution of 110-km from FC's and FD's 280 km.

Since ISCCP-FC and FD products were released, they have been used worldwide by researchers in numerous research studies and have inspired/promoted a number of new avenues in cloud-radiation research. The following are a few of examples for most important applications of ISCCP flux data in several research areas based on work by various authors.

(1) Validation/evaluation and comparison studies for radiative flux datasets.

All datasets are subject to some kind of validation/evaluation before they can become useful. As stated above, the uncertainty estimates for ISCCP flux products are obtained through various validation/evaluation procedures. Similarly, other radiative flux products need go through such processing by comparing them with various observed fluxes (such as GEBA, BSRN) and observation-based-calculated flux products such as ISCCP, and GEWEX-SRB (Stackhouse et al., 2011). Indeed, there have been extensive uses of the ISCCP flux datasets by various authors that have promoted the improvements of both climatological data production and radiative models, e.g., Oreopoulos et al. (2012) have found our RadD-based atmospheric SW absorption has ~5 W/m^2 low bias in inter-comparison of about a dozen of radiation models with identical input datasets; the finding led to our improvement for RadH, Another example is that CERES has improved its Angular Distribution Models (ADM) for Top-of-Atmosphere radiative flux estimation (Loeb et al., 2007) over the ADM of ERBE (see, e.g., Barkstrom and Smith, 1986) as inaccuracies of ERBE's ADM were pointed out by many authors, including Rossow and Zhang (1995). The most comprehensive flux assessment activities were organized by WCRP GEWEX Radiative Flux Assessment (RFA) conducted over several years with more than a dozen of institutes and their datasets involved (see Raschke, et al., 2012a and 2012b). The RFA activities have benefited all the participated institutes in improving their flux datasets.

(2) Sensitivity study of flux calculation to atmospheric and surface physical properties or models.

In radiative flux calculation, there are many physical parameters to represent, such as sun's spectral incoming flux intensity at TOA, radiative properties of atmospheric constituents (gases, aerosols, etc.), atmospheric temperature and humidity, macrophysical and microphysical properties of clouds (morphology, particle size, phase, etc.), surface properties (albedo, temperature, etc.) that are imported to a radiation model to produce total flux results (broadband SW and LW fluxes). This means that we can relatively easily quantify the radiative flux changes due to changes of individual (or group of) properties by changing one or several physical input parameters or even atmospheric structure and model's parameterization in the flux calculations to diagnose their

respective influences on flux results that would help understand their separate roles in the radiative energy distribution in the earth-atmosphere system. Because in the real world we can only measure the total flux results, it is difficult to separate the radiative flux components according to their individual contributions and properties. Sensitivity studies have provided a powerful tool to estimate the roles of individual contributions of physical properties and how they affect the radiative fluxes or cooling/heating rates in the atmosphere, ocean and land, etc. Furthermore, the calculated fluxes are not without errors or uncertainties since there are always uncertainties/errors coming with input datasets and even the radiation model itself. Accordingly, the sensitivity test is also useful to break down how and how much these errors/uncertainties are caused by different components, either from input variables or from radiation modeling so as to improve the input data and radiation model in order to have more accurate flux results. We have systematically conducted various sensitivity tests on ISCCP radiation fluxes, e.g., Table 2 in Zhang et al. (1995) shows a list of typical sensitivity tests for ISCCP-FC; also see Zhang et al. (2004, 2006 and 2007a) and Chen et al. (2000a and 2000b).

The methodology of (1) and (2) has been substantially generalized and widely used over the past two decades in the Model Inter-comparison Projects (MIP or MIPS) for different Global Circulation Models (GCMs), as well as for other climate and radiation models such as RFMIP (for Radiation Forcing, see, e.g., Piers et al., 2016), CMIPS (for Climate, see, e.g., Eyring et al., 2015)), CFMIP (for Cloud Feedback, see, e.g., Webb et al., 2017), etc. These inter-comparisons have been invaluable for model and climatological feedback evaluation and for a better understanding of climate modeling and improving its prediction capabilities.

(3) Earth radiation balance and budget at TOA and surface.

Our earth-atmosphere system has been in a quasi-equilibrium state for geologically long-time period with a fluctuation within a moderate temperature range (e.g., 0.8 million years, as described in Hansen and Sato, 2011, https://www.giss.nasa.gov/research/briefs/hansen_15/PaleoImplications.pdf). It is under such quasi-equilibrium conditions, that the human beings and other living things have been able to survive. Since the earth-atmosphere system's energy source is the sun alone, while the system's energy sink is only through thermal radiation at TOA (OLR for Outgoing Longwave Radiation) emitted to outer space, the TOA incoming SW and OLR fluxes must be approximately balanced in order to maintain such a quasi-equilibrium state. In other words, the earth radiation budget's balance at TOA is fundamentally vital for all the life on Earth, and thus has been long drawn scientific interest since Simpson (1929). As the radiation budget at TOA and the surface of earth are closely related, it is no wonder that the ISCCP-FD results have been widely used for the radiation budget studies at both TOA and surface, see, e.g., Ohmura (2014), Trenberth et al. (2009), Wong et al. (2006) and Loeb et al. (2009). Furthermore, how can the earth-atmosphere system be maintained to have at such a status for such a long period that has not been possible on the other planets? Can this status be destroyed by today's increasing human activities or natural disasters? All such important scientific questions are what the climatologists and other scientists now working on in order to address and answer them.

(4) Global energy transports and the derivation of surface turbulence fluxes.

The differential distribution of the TOA total net flux with latitude can be used to derive the required global meridional total energy transport (see, e.g., Carissimo et al., 1985). The total energy transport of the earth-atmosphere system can be partitioned into atmosphere and ocean as shown in Peixoto and Oort (1992). Zhang and Rossow (1997) suggested using the boundary fluxes, i.e., surface radiative and turbulent fluxes, to do such partitioning instead of direct measurement in the atmosphere or/and ocean which prompted SeaFlux projects, in which, turbulent fluxes are produced (see, e.g., Curry et al., 1999; Curry et al., 2004, Yu and Weller, 2007). Our earth-atmosphere system is similar to a (low-efficiency) heat engine that takes input energy from the Sun (SW flux) to drive all kinds of dynamic processes in the system and expel the energy through OLR, which is exactly what the General Circulation Model (GCM) has been developed for in order to simulate to study all the dynamic processes in the system, including global energy transport and how turbulence affects planetary boundary layer.

(5) Long-term energy trends and variations of the atmosphere-earth system

As human beings, we are concerned about how long the current climate system can be maintained in its quasi-equilibrium status that enables human beings to survive. The temporal variations of the TOA radiation budget is what the climatologists have been working on in order to study long-term energy trends and variations of the atmosphere-earth system and to refine the ability to predict the future climate change, see, e.g., Hansen et al. (1997), Romanou et al.(2007), Zhang et al. (2007b), Wong et al. (2006).

In short, the above incomplete list of research has shown how important a good flux product can be.The ISCCP-based flux products like ISCCP-FH (and GEWEX-SRB) are especially valuable because there is no other product that has global coverage and minimum-required diurnal sampling (eight times a day) with temporal coverage period longer than ISCCP period of 34 years.

In the following slides, we focus on the fundamental features of the current ISCCP-FH Radiative Profile Flux Production and its validation/evaluation. We provide some necessary comparisons with other products, past and present, so that readers can understand how it has been developed and what its current status and uncertainty estimates are.

The slides begin with an overall background introduction (slides 2 – 3) and outline (slides 4 – 9) for the ISCCP-FH product, and then give a description of overall improvements of ISCCP-FH (slides 7 – 11) and specific, important improvements (slides 10 – 12). Slides 13 – 16 compare fluxes of ISCCP-FH and FD with CERES at TOA and in the atmosphere, respectively, and 17 – 18 are for surface validation for ISCCP-FH (and FD and CERES) against BSRN. The last two slides (19 – 20) provide an overall uncertainty estimate of ISCCP-FH and conclusions, respectively.

Acknowledgments

We would like to give special thanks to Dr. Reto Reudy who helped separate the radiation code (RadE) from NASA GISS GCM ModelE that makes possible to initiate the ISCCP-FH project. We thank Dr. Stefan Kinne who has provided us with Aerocom, MACv1 and MACv2 aerosol datasets. We also thank Dr. Paul W. Stackhouse and Dr. Shashi K. Gupta who have provided us with TSI datasets. Computer facilities are supplied by NOAA's National Centers for Environmental Information and NASA GISS/Columbia University. The development of the ISCCP-FH production code was funded by NOAA Climate Data Record Project (Grant NA11NES4400002 for 2011 – 2014). Finally we thank CERES, BSRN, CloudSat and CALIPSO teams for providing us with their datasets for the ISCCP-FH project's development and validation work.

References

Barkstrom B. R. and G. L. Smith (1986), the Earth Radiation Budget Experiment: Science and implementation, Rev. Geoph., V. 24, No. 2, 379-390, 1986.

Cess, R. D. and I. L. Vulis (1989), Inferring surface solar absorption from broadband satellite measurements, Journal of Climate, Vol. 2, No. 9, 1989

Chen, Ting, W. B. Rossow and Y.-C. Zhang (2000a), Radiative effects of cloud type variations, *J. Clim., Vol. 13,* 264-286.

Chen, Ting, Y.-C. Zhnag and W. B. Rossow (2000b), Sensitivity of atmospheric radiative heating rate profiles to variations of cloud layer overlap, *J. Clim., Vol. 13,* 2941-2959.

Carissimo, B. C., A. H. Oort, and T. H. Vonder Haar, 1985: Estimating the meridional energy transports in the atmosphere and ocean. *J. Phys. Oceanogr.,* **15,** 82–91.

Curry, J. A., C. A. Clayson, W. B. Rossow, R. Reeder, Y. C. Zhang, P. J. Webster, G. Liu, and R. S. Sheu (1999), High-resolution satellite-derived dataset of the ocean surface fluxes of heat, freshwater and momentum for the TOGA COARE IOP. *Bull. Amer. Meteor. Soc.,* 80**,** 2059–2080.

Curry, J., and coauthors (2004), SeaFlux, *Bull. Amer. Meteor. Soc., 85*, 409-424.

DeAngelis, Anthony M., X. Qu, M.D. Zelinka and A. Hall (2015), An observational radiative constraint on hydrologic cycle intensification, Nature, V. 528, 249-253, doi:10.1038/nature15770

Eyring, V., S. Bony, G.A. Meehl, C. Senior, B. Stevens, R.J. Stouffer and K.E. Taylor, Overview of the Coupled ModelIntercomparison Project Phase 6 (CMIP6)experimental design and organization, Geosci. Model Dev. Discuss., 8, 10539–10583, 2015, doi:10.5194/gmdd-8-10539-2015.

Fu, Q., K.N. Liou, M.C. Cribb, T.P. Charlock, and A. Grossman, 1997: Multiple scattering parameterization in thermal infrared radiative transfer. J. Atmos. Sci., 54, 2799-2812.

Hagihara, Y., H. Okamoto, and R. Yoshida (2010), Development of a combined CloudSat‐CALIPSO cloud mask to show global cloud distribution, J. Geophys. Res., 115, D00H33, doi:10.1029/2009JD012344.

Hagihara, Y., H. Okamoto, and Z. J. Luo (2014), Joint analysis of cloud top heights fromCloudSat and CALIPSO: New insights into cloud top microphysics, J. Geophys. Res. Atmos., 119, 4087–4106, doi:10.1002/2013JD020919.

Hansen, J. et al. (1983), Efficient three-dimensional global models for climate studies: Model I and II, Mon. Weather Rev., 111, 609– 662.

Hansen, J., et al., Climate forcings in Goddard Institute for Space Studies SI2000 simulations, J. Geophys. Res., 107(D18), 4347, doi:10.1029/2001JD001143, 2002.

Kelley, M., Schmidt, G. A., Nazarenko, L. S., Bauer, S. E., Ruedy, R., Russell, G. L., et al. (2020). GISS‐E2.1: Configurations and climatology. Journal of Advances in Modeling Earth Systems, 12, e2019MS002025. https://doi.org/10.1029/2019MS002025.

Kinne, S., D. O'Donnel, P. Stier, S. Kloster, K. Zhang, H. Schmidt, S. Rast, M. Giorgetta, T. F. Eck, and B. Stevens (2013), MAC-v1: A new global aerosol climatology for climate studies, J. Adv. Model. Earth Syst., 5, 704–740, doi:10.1002/jame.20035.

Lacis, A.A., and V. Oinas (1991), A description of the correlated k distributed method for modeling nongray gaseous absorption, thermal emission, and multiple scattering in vertically inhomogeneous atmospheres. J. Geophys. Res., 96, 9027-9063, doi:10.1029/90JD01945.

Loeb, N.G., S. Kato, K. Loukachine, N Manalo-Smith and D. R. Doelling (2007), Angular distribution models for top-of-atmosphere radiative flux estimation from the Clouds and the Earth's Radiant Energy System instrument on the Terra satellite. Part II: Validation. J. Atmos. Ocean. Technol. **2007**, 24, 564–584, 2007.

Loeb, N. G., W. B. A. Wielicki, D. R. Doelling, G. L. Smith, D. F. Keyes, S. Kato, N. Manalo-Smith, and T. Wong (2009), Toward Optimal Closure of the Earth's Top-of-Atmosphere Radiation Budget, J. Clim., V. 22, 748-766, 2009.

Ma, Y., and R. T. Pinker (2012), Modeling shortwave radiative fluxes from satellites, J. Geophys. Res. 117, D23202,doi:10.1029/2012JD018332.

Ohmura, A., and H. Gilgen (1991), The GEBA data base, interactive applications, retrieving data, Rep. 2, 60 pp., Global Energy Balance Arch., World Clim. Program Water Proj. A7, Zu¨ rich.

Ohmura, A., et al. (1998), Baseline Surface Radiation Network (BSRN/WCRP): New precision radiometry for climate research, Bull. Am. Meteorol. Soc., 79, 2115– 2136.

Ohmura, A. (2014), The Development and the Present Status of Energy Balance Climatology, J. *Meteor. Soc. Japan*, Vol. 92, No. 4, pp. 245−285, 2014, DOI:10.2151/jmsj.2014-401

Oreopoulos, L., et al. (2012), The Continual Intercomparison of Radiation Codes: Results from Phase I, J. Geophys. Res., 117, D06118, doi:10.1029/2011JD016821.

Pincus, R., P.M. Forster and B. Stevens (2016), The Radiative Forcing Model Intercomparison Project (RFMIP): experimental protocol for CMIP6, Geosci. Model Dev., 9, 3447–3460, 2016, doi:10.5194/gmd-9-3447-2016.

Pinker, R. T., and I. Laszlo (1992), Modeling surface solar irradiance for satellite application on a global scale, J. Appl. Meteorol., 31, 194– 211, doi:10.1175/1520-0450(1992)031<0194:MSSIFS>2.0.CO;2.

Peixoto, J. P., and A. H. Oort, 1992: *Physics of Climate,* AIP, 520 pp.

Raschke, E., S. Kinne, P.W. Stackhouse (leading authors) etal., (2012a), GEWEX Radiative Flux Assessment (RFA) Volume 1: Assessment, A Project of the World Climate Research Programme Global Energy and Water Cycle Experiment (GEWEX) Radiation Panel, WCRP Report No. 19/2012.

Raschke, E., S. Kinne, P.W. Stackhouse (leading authors) etal., (2012b), GEWEX Radiative Flux Assessment (RFA) Volume 2: Supplementary, InformationA Project of the World Climate Research Programme Global Energy and Water Cycle Experiment (GEWEX) Radiation Panel, WCRP Report No. 19/2012.

Romanou, A., B. Liepert, G. A. Schmidt, W. B. Rossow, R. A. Ruedy, and Y. Zhang (2007), 20th century changes in surface solar irradiance in simulations and observations, Geophys. Res. Lett., 34, L05713, doi:10.1029/2006GL028356.

Rossow, W. B. and R. A. Schiffer (1999), Advances in understanding clouds from ISCCP, B. Am. Meteorol. Soc., 80, 2261–2288, https://doi.org/10.1175/1520-0477(1999)080<2261:AIUCFI>2.0.CO;2, 1999.

Rossow, W.B., and A.A. Lacis (1990), Global, seasonal cloud variation from satellite radiance measurements, 2, Cloud properties and radiative effects, J. Climate, 3, 1204-1253, 1990.

Rossow, W.B., and R.A. Schiffe (1991), ISCCP cloud data products. *Bull. Amer. Meteor. Soc.,* **72,** 2-20.

Rossow, W. B., and Y.-C. Zhang (1995), Calculation of surface and top of atmosphere radiative fluxes from physical quantities based on ISCCP data sets: 2. Validation and first results, J. Geophys. Res., 100, 1167–1197.

Rossow, W. B., A. W. Walker, D. Bueschel, and M. Roiter (1996), International Satellite Cloud Climatology Project (ISCCP) documentation of new cloud datasets, WMO/TD-737, 115 pp., World Clim. Res. Programme, Geneva, Feb.

Rossow, W.B., and Y.-C. Zhang (2010), Evaluation of a statistical model of cloud vertical structure using combined CloudSat and CALIPSO cloud layer profiles. J. Climate, 23, 6641-6653, doi:10.1175/2010JCLI3734.1

Rothman, L.S. and coauthors, 2013, The HITRAN2012 molecular spectroscopic database, *J. Quantitative Spectroscopy & Radiative Transfer, 130(2013), 4-50.*

Schiffer, R.A., and W.B. Rossow (1983), The International Satellite Cloud Climatology Project (ISCCP): The first project of the World Climate Research Program. *Bull. Amer. Meteor. Soc.,* **64,** 779-784.

Schmidt, G.A., R. Ruedy, J.E. Hansen, I. Aleinov, N. Bell, M. Bauer, S. Bauer, B. Cairns, V. Canuto, Y. Cheng, A. Del Genio, G. Faluvegi, A.D. Friend, T.M. Hall, Y. Hu, M. Kelley, N.Y. Kiang, D. Koch, A.A. Lacis, J. Lerner, K.K. Lo, R.L. Miller, L. Nazarenko, V. Oinas, J.P. Perlwitz, J. Perlwitz, D. Rind, A. Romanou, G.L. Russell, M. Sato, D.T. Shindell, P.H. Stone, S. Sun, N. Tausnev, D. Thresher, and M.-S. Yao (2006), Present day atmospheric simulations using GISS ModelE: Comparison to in-situ, satellite and reanalysis data. *J. Climate*, 19, 153-192, doi:10.1175/JCLI3612.1.

Simpson, G. C.(1929), The distribution of terrestrial radiation, Mem. R. Meteorol. Soc., 3, 53-78, 1929.

Stephens, G.L., Deborah G. Vane, Ronald J. Boain, Gerald G. Mace, Kenneth Sassen, Zhien Wang, Anthony J. Illingworth, Ewan J. O'Connor, William B. Rossow, Stephen L. Durden, Steven D. Miller, Richard T. Austin, Angela Benedetti, Cristian Mitrescu, and the CloudSat Science Team (2002), The CloudSAT mission and the A-train, A New Dimension of Space-Based Observations of Clouds and Precipitation, *Bull. Amer. Meteor. Soc., Vol. 83, No. 12, December, 2002.*

Stackhouse, Jr., Paul W., Shashi K. Gupta, Stephen J. Cox, J. Colleen Mikovitz, Taiping Zhang, and Laura M. Hinkelman, 2011: The NASA/GEWEX Surface Radiation Budget Release 3.0: 24.5-Year Dataset. GEWEX News, 21, No. 1, February, 10-12.

Stockholm (1975), The physical basis of climate and climate modeling. *GARP Publ. Ser. 16*, World Meteorological Organization, Geneva.

Trenberth, Kevin E., John T. Fasullo, and Jeff rey Kiehl (2014), Earth's global energy budget, *Bull. Amer. Meteor. Soc., March, 2009. 311-323.*

Wang, J., W. B. Rossow, and Y.-C. Zhang (2000), Cloud vertical structure and its variations from 20-yr global rawinsonde dataset, J. Clim., 12, 3041–3056.

Webb, M.J. and coauthors (2017), The Cloud Feedback Model Intercomparison Project (CFMIP) contribution to CMIP6, Geosci. Model Dev., 10, 359–384, 2017, doi:10.5194/gmd-10-359-2017.

Wielicki, B. A., B. R. Barkstrom, E. F. Harrison, R. B. Lee, G. L. Smith, and J. E. Cooper (1996), Clouds and the Earth's Radiant Energy System (CERES): An Earth Observing System experiment, Bull. Am. Meteorol. Soc., 77, 853– 868.

Wong, T., B. A. Wielicki, and R. B. Lee III (2006), Reexamination of the Observed Decadal Variability of the Earth Radiation Budget Using Altitude-Corrected ERBE/ERBS Nonscanner WFOV Data, J. Clim,, Vol. 19, 2006, 4028-4040.

Young, A. H., K. R. Knapp, A. Inamdar, W. Hankins, and W. B. Rossow (2018), The International Satellite Cloud Climatology Project H-Series climate data record product, Earth Syst. Sci. Data, 10, 583-593, https://doi.org/10.5194/essd-10-583-2018, 2018.

Yu, Lisan and R. A. Weller (2007), Objectively Analyzed Air–Sea Heat Fluxes for the Global Ice-Free Oceans (1981–2005), *Bull. Amer. Meteor. Soc., 88***,** 527-539.

Zhang, Y.-C., W.B. Rossow and A. A. Lacis (1995), Calculation of surface and top of atmosphere radiative fluxes from physical quantities based on ISCCP data sets, 1. Method and sensitivity to input data uncertainties, J. Geophys. Res., 100, 1149-1165, 1995.

Zhang, Y-C., W.B. Rossow, A.A. Lacis, M.I. Mishchenko and V. Oinas (2004),
Calculation of radiative fluxes from the surface to top-of-atmosphere based on ISCCP and other global datasets: Refinements of the radiative transfer model and the input data. J. Geophys. Res., 109, doi 10.1029/2003JD004457 (1-27 + 1-25), 2004.

Zhang, Y., W. B. Rossow, and P. W. Stackhouse Jr. (2006), Comparison of different global information sources used in surface radiative flux calculation: Radiative properties of the near-surface atmosphere, J. Geophys. Res., 111, D13106, doi:10.1029/2005JD006873.

Zhang, Y., W. B. Rossow, and P. W. Stackhouse Jr. (2007a), Comparison of different global information sources used in surface radiative flux calculation: Radiative properties of the surface, J. Geophys. Res., 112, D01102, doi:10.1029/2005JD007008.

Zhang, Y., W. B. Rossow, P. Stackhouse Jr., A. Romanou, and B. A. Wielicki (2007b), Decadal variations of global energy and ocean heat budget and meridional energy transports inferred from recent global data sets, J. Geophys. Res., 112, D22101, doi:10.1029/2007JD008435.

Slide 1

Calculation, Evaluation and Application of Long-term, Global Radiative Flux Datasets at ISCCP: Past and Present

Yuanchong Zhang[1,3,4], William B. Rossow[2], Andrew A. Lacis[3] and Valdar Oinas[4]

[1]Columbia University; [2] CCNY; [3]NASA GISS; [4] SciSpace, LLC

Slide 2

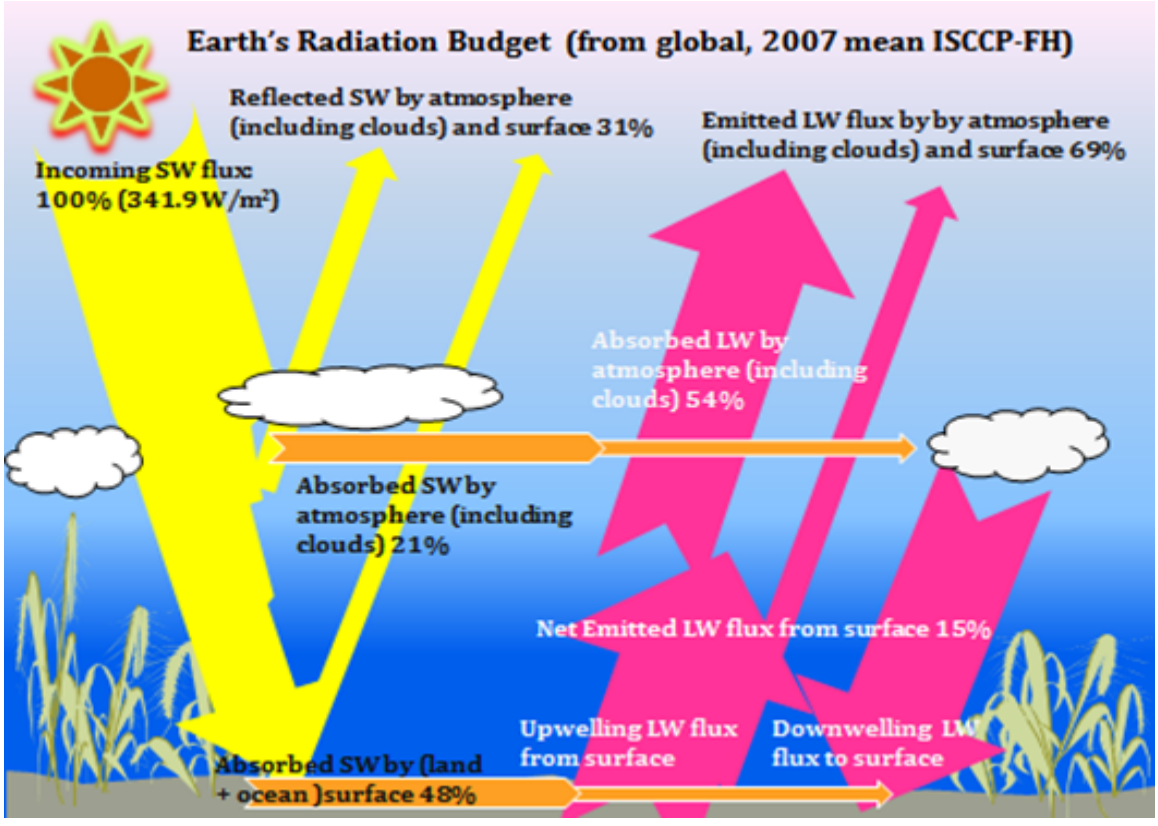

Slide 3

Why ISCCP FLUX Calculation?

1. To understand the fundamental earth radiation and energy budget problem and answer how the quasi-equilibrium status of the earth-atmosphere system can be maintained.
2. To evaluate this and other flux products.
3. To improve input datasets and radiation models.
4. To study cloud radiative effects (cloud forcing), energy transport, local or regional radiation/energy balance, etc.
5. To produce surface turbulence fluxes
6. To study long-term trends of earth radiation/energy budget.
7. To estimate solar energy for solar-electric panels.

Slide 4

Evolution of the ISCCP Flux Products Through Three Generations

Flux Product Name	ISCCP-FC	ISCCP-FD	ISCCP-FH
Beginning Year	1995	2003	2017
Reference for flux data	Zhang et al. 1995	Zhang et al., 2004	TBD
Main input datasets	ISCCP-C	ISCCP-D	ISCCP-H
Vertical resolution	at TOA and Surface	5-level ATM profile	5-level ATM profile
Horizontal resolution	280 km	280 km	110 km
Temporal resolution	3 hourly	3 hourly	3 hourly
Temporal coverage	1985-1989	1983-2009	1983-2009-onward
Uncertainty at TOA	10 – 15 W/m^{-2}	5 – 10 W/m^{-2}	$\lesssim$ 10 W/m^{-2}
Uncertainty at Surface	20 - 25 W/m^{-2}	10 - 20 W/m^{-2}*	$\lesssim$ 10 - 20 W/m^{-2}
Radiation code	RadII	RadD	RadH
Based GISS GCM model	Model II	ModelD/SI2000	ModelE
GCM References	Hansen et al., 1983	Hansen et al., 2002	Schmidt et al., 2006

**Originally it is 10 - 15 W/m^{-2}, as reported in Zhang et al. (2004) based on limited validation; but 10 – 20 W/m^{-2} may better reflect the truth based on more validation.*

Slide 5

Main Radiation-model Improvements of ISCCP-FH

- **Based on** RadH, improved/revised from RadE, the radiation code of the GISS ModelE (of 2011), vs. RadD, revised from GISS Model SI2000 or ModelD (of 2002)
- **Spectral resolution** in k's (for Correlated K-distribution method): Improved
  reformulated/updated 16 k's for SW (0.2 - 5.0 μm) [though same 16 k's in FD]
  reformulated/updated 33 k's LW (5.0 -200.0 μm) [though same 33 k's in FD]
- **Spatial resolution**: 110 km [vs. 280 km in FD]
- **Accuracy**: same 1 W/m^2 and 1% cooling rates at TOA and SRF for LW and SW, respectively, but with significant reformulation and updates, especially atmospheric gas absorption and elaboration of LW calculation w.r.t. ISCCP-FD.
- **Reformulation of Atmospheric Gases for SW calculation**:
  Added weak line absorption for H2O, O2 and CO2, and updated line absorption for CH4, N2O, etc., which has virtually removed low bias of atmospheric absorption.
- **Reformulation/Refining for LW calculation**:
  RadH has several improvements for LW flux calculation over RadD, including additional Ma2008 option and MT-CKD H2O continua options (vs. RadD's sole Ma2000 scheme), CFC absorption cross-section, SO2 line absorption and better treatment of CH4 and N2O overlap with major absorbers with HITRAN2012 atlas, if possible.
  In addition, RadH increases the base atmospheric vertical resolution using a 43-layer standard atmosphere (old 24 layers), and now takes into account of amount of water vapor above and below a given layer as well as the water vapor gradient.

Slide 6

Contents of the ISCCP-FH Product

► It is a SuRFace (SRF)-to-TOA, 5-level, flux profile product:

- FH stands for: Flux profile data calculated (mainly) using ISCCP **H** series data to replace its precursor = ISCCP-**FD** (2003, final coverage: 8307-0912)
- Spectral coverage: 0.2 – 200 μm (SW: 0.2 – 5.0 and LW: 5.0 – 200)
- Spatial resolution: horizontal: 110km equal-area (1.0° on equator)
  vertical: 5 levels (SRF-680mb-440mb-100mb-TOA)
- Temporal resolution: 3-houly (UTC = 0, 3, … 21)
- Spatial coverage: virtually fully global
- Temproal coverage: July 1983 – June 2017 (and onwards)

► Outputs are compiled into five sub-products:

(1) **FH-TOA** Top-Of-Atmosphere radiative fluxes (23 variables)
(2) **FH-SRF** SuRFace Radiative Fluxes (34 var's)
(3) **FH-PRF** 5-level PRoFile Radiative Fluxes (including TOA and SRF, 91 var's))
(4) **FH-MPF** Monthly mean of FH-PRF (same 91 var's)
(5) **FH-INP** Complete INPut dataset (up to a maximum of 335 var's)

– ***All are available at:*** https://isccp.giss.nasa.gov/projects/flux.html
in NetCDF except FH-INP only in Binary for July 1983 to June 2017.

Slide 7

Summary of Input Dataset for ISCCP-FH Production

(1) Atmospheric Gases: Climatology from NASA GISS radiation code of ModelE

(2) Atmospheric temperature/humidity Profile: nnHIRS (in HGG) vs TOVS in D1

(3) Atmospheric aerosol climatology: MACv2 (Stefan Kinne, MPI-Meteorology)

(5) Clouds: ISCCP-HGG (18 types vs 15 types in ISCCP-D1)

(6) Particle size of liquid/ice clouds based on Han et al. (1994) climatology

(7) Surface air temperature: from ISCCP-HGG (of nnHIRS); in addition, RadH makes cloud-caused, diurnal adjustment on it for land areas (> 1/3 fraction) using climatology from NCEP & NMC Surface Weather station reports

(8) Surface skin temperature: from SCCP-HGG; RadH also makes additional cloud-caused, diurnal-adjustment (for land)

(9) Surface albedo: MACv2-aerosol-corrected reflectance for 0.55 μm from non-aerosol-corrected (processed based on ISCCP-HXG), modulated using VIS/NIR of revised RadE to have broadband albedo (for six wavebands)

(10) O3, Snow/Ice, vegetation and other surface characteristic (type, topography, land ice, etc.) data: from ISCCP-H Ancillary data

(11) TSI (total solar irradiance): self-consistent daily time series based on SORCE V-15, Davos WRC composite and RMIB (from Dr. Shashi Gupta).

Slide 8

Summary of Output Variables in ISCCP-FH Product

(1) Radiative Flux Profile:

Full-sky SW↑, SW↓, LW↑, LW↓ (and direct/diffuse downward at SRF)

Clear-sky SW↑, SW↓, LW↑, LW↓ (and direct/diffuse downward at SRF)

100% overcast SW↑, SW↓, LW↑, LW↓ (and direct/diffuse downward at SRF)

at 5 levels:

TOA ——— (~ 100 km high)

100 mb ———

440 mb ———

680 mb ———

Surface ——— (Ground ≤ 1100 mb)

} **Flux Profile**

(2) Input data Variables:

- Summary input variables for **TOA, SRF, PRF** and **MPF** sub-products
- ~Complete inputs for **INP** sub-product that may be used to reproduce FH

Slide 9

Comparison of main Global, Long-term flux products

Feature	CERES (Level 3) (SYN1deg Edition3A)	GEWEX-SRB (v3.1LW/3.0SW)	ISCCP-FH (v 0.00)
Cover Period	2000 – current	1983 – ISCCP-D/H's current	1983 – ISCCP-H's current
Spatial Reso	1° x 1°	1° x 1°	1° x 1° (110 km EQ)
Temporal Reso	3-hourly	3-hourly	3-hourly
TOA flux	yes (observed + calculated)	yes (calculated)	yes (calculated)
SRF flux	yes (calculated)	yes (calculated)	yes (calculated)
In-Atmosphere Flux (Profile)	Yes, 3 levels: 70, 200 and 500 mb	No	Yes, 3 levels: 100. 440 and 680 mb
SW: algorithm based on	Various (http://ceres.larc.nasa.gov/atbd.php)	Pinker and Laszlo (1992)	Correlated K-distribution (Schmidt et al., 2006)
LW: algorithm based on		Fu et al. (1997)	
PAR/UV index	Yes	PAR	No

Slide 10

Improvement by New MACv2 Aerosol Climatology: Example

(Name & location of 10 Surface Stations are show on Slide 17 in Red color)

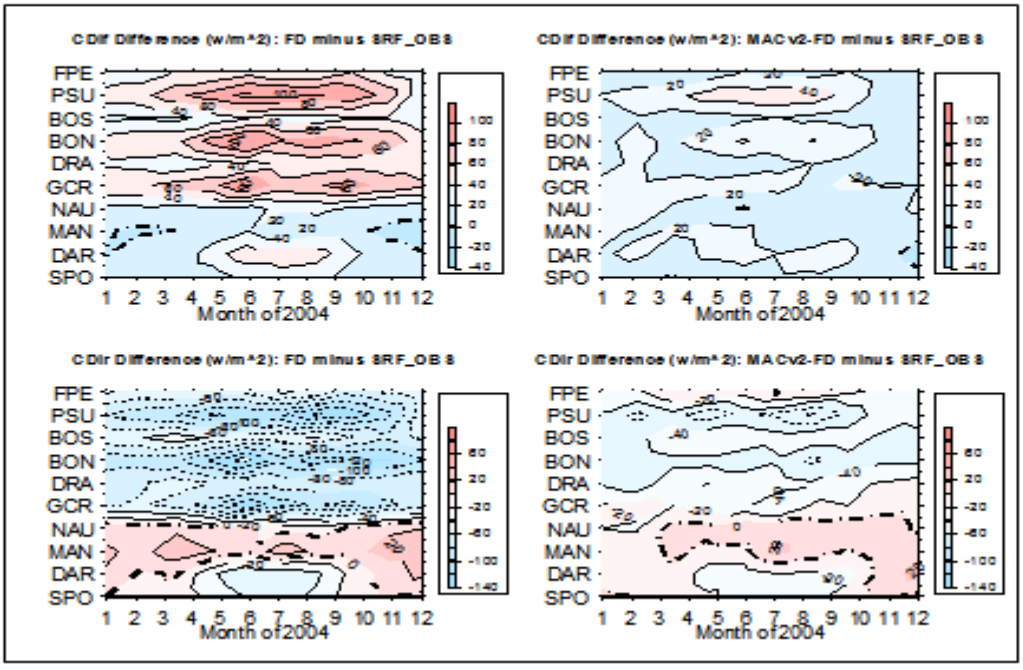

Slide 11

Improvement by New Vertical Cloud Layer Configuration (VCLC)

- **VCLC consists of (1) CVS and (2) CLTC**

(1). CVS (Cloud Vertical Structure): Model B for FH (18 cloud types)

Layer	ISCCP-H Cloud Class	Sub-class	Vertical structure	How to construct
HC	Ci		1H	= single layer cloud
	Cs	Thin	HM*	Radiatively reconstructed
		Thick	HML	ISCCP Clim reconstructed
	Cb		1 H-M-L	ISCCP Clim reconstructed
MC	Ac	Thin	1M	= single layer cloud
		Thick	HL*	Radiatively reconstructed
	As	Thin		
		thick	ML	ISCCP Clim reconstructed
	Ns			
LC	Cu		1L	= single layer cloud
	Sc			
	St			

(2). CLTC (Cloud Layer Thickness Configuration):

-- **Function of Cloud optical thickness (τ), Longitude, Latitude & Ocean/Land**

Based on 20-yr Rawinsonde and 5-yr CloudSat-CALIPSO climatology

Slide 12

Improvement by new VCLC: Example

Vertical Cloud Fraction Profile: 0707 Ocean & Land

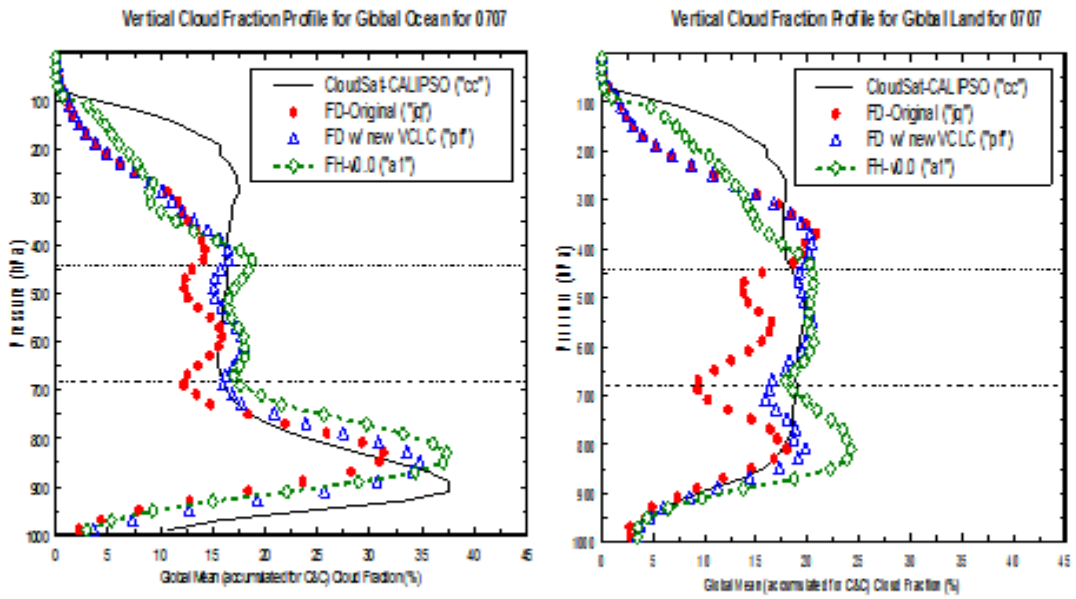

Slide 13

Preliminary validation against CERES for 2017 Monthly means: All-sky at TOA

All-sky ISCCP-FH vs CERES at TOA

Variable	FH mean	CERES mean	Mean diff	Stdv	cor coef	Slope	intrcept	Nrm dev	Eq cell #
ALBEDO (%)	33.64	31.48	2.153	3.413	0.9691	0.95	-0.60	2.43	485291
SW_net (W/m²)	235.56	242.61	-7.054	8.455	0.9970	1.00	6.66	5.97	494824
LW_net (W/m²)	-232.11	-239.18	7.071	4.560	0.9912	1.00	-6.62	3.22	494824
SW_ce (W/m²)	-49.52	-47.16	-2.359	10.261	0.9572	0.92	-1.45	7.27	494599
LW_ce (W/m²)	26.95	26.76	0.189	6.124	0.9305	0.98	0.37	4.37	485960

All-sky ISCCP-FD vs CERES at TOA

Variable	FD mean	CERES mean	Mean diff	Stdv	cor coef	Slope	intrcept	Nrm dev	Eq cell #
ALBEDO (%)	34.13	31.64	2.489	3.718	0.9627	1.00	-2.47	2.63	77842
SW_net (W/m²)	234.57	242.57	-8.000	8.577	0.9969	1.01	5.54	5.98	79152
LW_net (W/m²)	-236.10	-239.16	3.061	4.876	0.9899	1.01	-0.50	3.42	79152
SW_ce (W/m²)	-52.78	-47.15	-5.631	8.182	0.9763	0.90	0.13	5.40	79152
LW_ce (W/m²)	26.88	26.94	-0.059	4.884	0.9574	0.93	2.00	3.47	79063

Slide 14

Preliminary validation against CERES for 2017 Monthly means: Clear-sky at TOA

Clear-sky ISCCP-FH vs CERES at TOA

Variable	FH mean	CERES mean	Mean diff	Stdv	cor coef	Slope	intrcept	Nrm dev	Eq cell #
ALBEDO (%)	18.95	17.16	1.789	4.325	0.9519	0.90	0.12	3.04	484911
SW_net (W/m²)	285.15	289.85	-4.698	10.977	0.9961	0.99	7.75	7.75	494671
LW_net (W/m²)	-259.45	-266.32	6.877	6.183	0.9828	1.03	1.74	4.23	486037

Clear-sky ISCCP-FD vs CERES at TOA

Variable	FD mean	CERES mean	Mean diff	Stdv	cor coef	Slope	intrcept	Nrm dev	Eq cell #
ALBEDO (%)	18.56	17.30	1.261	3.620	0.9630	0.98	-0.81	2.58	77752
SW_net (W/m²)	287.35	289.72	-2.369	8.191	0.9979	0.99	5.15	5.76	79152
LW_net (W/m²)	-262.97	-266.10	3.126	6.474	0.9802	0.99	-5.58	4.60	79063

Slide 15

Preliminary validation against CERES for 2017 Monthly means: In atmosphere all-sky

All-sky ISCCP-FH vs CERES in Atmosphere

Variable	FH mean	CERES mean	Mean diff	Stdv	cor coef	Slope	intrcept	Nrm dev	Eq cell #
SW_net (W/m²)	76.60	78.02	-1.412	8.008	0.9687	1.02	0.26	5.61	494824
LW_net (W/m²)	-178.25	-183.40	5.157	17.801	0.8823	0.69	-59.78	11.27	494824
SW_ce (W/m²)	2.61	2.15	0.460	7.456	0.3515	0.78	0.12	5.85	494599
LW_ce (W/m²)	5.91	1.10	4.816	11.248	0.8835	1.01	-4.89	7.90	485960

All-sky FISCCP-FD vs CERES in Atmosphere

Variable	FD mean	CERES mean	Mean diff	Stdv	cor coef	Slope	intrcept	Nrm dev	Eq cell #
SW_net (W/m²)	71.76	78.00	-6.240	10.167	0.9512	1.08	0.34	6.72	79152
LW_net (W/m²)	-185.08	-183.39	*-1.690*	18.118	0.7889	0.84	-28.06	13.48	79152
SW_ce (W/m²)	3.32	2.15	1.173	6.406	0.3724	0.61	0.13	5.30	79152
LW_ce (W/m²)	-4.48	0.95	-5.429	8.455	0.9367	0.94	5.18	6.07	79063

Slide 16

Preliminary validation against CERES for 2017 Monthly: In-atmosphere clear-sky

Clear-sky ISCCP-FH vs CERES in Atmosphere

Variable	FH mean	CERES mean	Mean diff	Stdv	cor coef	Slope	intrcept	Nrm dev	Eq cell #
SW_net (W/m²)	74.02	75.89	-1.873	8.002	0.9671	1.03	-0.03	5.56	494671
LW_net (W/m²)	-184.18	-184.59	0.407	17.024	0.9254	0.78	-40.86	11.05	486037

Clears-sky ISCCP-FD vs CERES in Atmosphere

Variable	FD mean	CERES mean	Mean diff	Stdv	cor coef	Slope	intrcept	Nrm dev	Eq cell #
SW_net (W/m²)	68.44	75.85	**-7.412**	9.173	0.9611	1.12	-0.97	5.70	79152
LW_net (W/m²)	-180.55	-184.30	3.752	18.951	0.8571	0.95	-13.56	13.71	79063

Slide 17

BSRN Stations used for Surface-flux Validation (39 are data-available for 2007)

Station	Lat	Lon	Station	Lat	Lon
1 ALE	82.49	297.58	21 DRA	36.626	243.982
2 EUR	79.989	274.060	22 BIL	36.605	262.484
3 NYA	78.925	11.930	23 E13	36.605	262.515
4 LER	60.139	358.815	24 TAT	36.058	140.126
5 TOR	58.254	26.462	25 GCR	34.255	270.127
6 LIN	52.210	14.122	26 BER	32.267	295.333
7 CAB	51.971	4.927	27 SBO	30.860	34.779
8 REG	50.205	255.287	28 TAM	22.790	5.529
9 CAM	50.217	354.683	29 KWA	8.720	167.731
10 PAL	48.713	2.208	30 NAU	-0.521	166.917
11 FPE	48.317	254.900	31 MAN	-2.058	147.425
12 PAY	46.815	6.944	32 COC	-12.193	96.835
13 CAR	44.083	5.059	33 DAR	-12.425	130.891
14 SXF	43.730	263.380	34 ASP	-23.798	133.888
15 PSU	40.720	282.067	35 LAU	-45.045	169.689
16 BOS	40.125	254.763	36 SYO	-69.005	39.589
17 BON	40.067	271.633	37 GVN	-70.650	351.750
18 BOU	40.050	254.993	38 DOM	-75.100	123.383
19 XIA	39.754	116.962	39 SPO	-89.983	335.201
20 CLH	36.905	284.287	*(Red-colored also for Slide 10 MACv2 test)*		

Slide 18

Preliminary validation against BSRN: for 2017 Monthly Mean

FLux	FH	BSRN	M. diff	Stdv	Cr coef	Slope	intrcept	Nrm dev	Stn #
SWdn (W/m²)	170.89	172.26	-1.369	20.911	0.9746	0.98	4.14	14.87	441
LWdn (W/m²)	302.52	310.00	-7.481	17.317	0.9770	0.96	20.34	12.26	458
SWup (W/m²)	56.92	67.87	-10.949	26.354	0.9543	1.09	6.01	17.29	89
LWup (W/m²)	287.18	289.15	-1.973	20.389	0.9755	1.09	-23.09	13.00	96

FLux	FD	BSRN	M. diff	Stdv	Cr coef	Slope	intrcept	Nrm dev	Stn #
SWdn (W/m²)	168.49	172.26	-3.772	23.820	0.9667	1.00	4.23	16.87	441
LWdn (W/m²)	320.25	310.00	10.249	21.508	0.9657	1.08	-37.45	14.00	458
SWup (W/m²)	44.53	67.87	-23.344	32.712	0.9281	1.11	18.56	21.31	89
LWup (W/m²)	289.68	289.15	0.534	19.080	0.9762	1.02	-7.71	13.25	96

FLux	CERES	BSRN	M. diff	Stdv	Cr coef	Slope	intrcept	Nrm dev	Stn #
SWdn (W/m²)	176.65	172.26	4.396	16.183	0.9848	1.00	-4.89	11.43	441
LWdn (W/m²)	304.98	310.00	-5.018	11.280	0.9899	0.99	6.95	7.99	458
SWup (W/m²)	57.27	67.87	-10.598	24.017	0.9598	1.02	9.69	16.82	89
LWup (W/m²)	282.13	289.15	-7.017	11.472	0.9923	1.04	-5.66	7.5	96

Slide 19

Preliminary Uncertainty Estimate for monthly/regional ISCCP-FH

(1) At TOA: for *Single flux component*: if taking CERES as 'truth'.
Bias $\lesssim$ 7 W/m^2 STDV $\lesssim$ 11 W/m^2
Corr coefficient $\geq$ 0.95 Normal Deviation $\lesssim$ 7 W/m^2
► Uncertainty $\lesssim$ 10 W/m^2
FH is comparable with but slightly worse than FD (but FH with higher spatial resolution) at TOA.

(2) At Surface: for *single flux component* based on Comparisons with BSRN:
Bias $\lesssim$ 11 W/m^2 STDV $\lesssim$ 26 W/m^2
Corr coefficient $\geq$ 0.95 Normal Deviation $\lesssim$ 17 W/m^2
► Uncertainty $\lesssim$ 15 - 20 W/m^2
-- FH is overall better than FD but slightly worse than CERES.

(3) In Atmosphere: for *Net and CE*,
Difference $\lesssim$ 5 W/m^2 STDV $\lesssim$ 18 W/m^2
Corr coefficient: 0.35 – 0.88 Normal Deviation $\lesssim$ 11 W/m^2
► Uncertainty $\lesssim$ 15 W/m^2
ISCCP-FH seems slightly better than FD, especially substantially improved in atmospheric SW-Net (absorption) based on comparison with CERES.

Slide 20

Conclusions

1. RadH represents the most recent improvements of the radiation code of the NASA GISS ModelE, especially in atmospheric gas absorption by SW and polar-region LW calculation, i.e., ISCCP-FH flux profile product is an improvement over its precursor, RadD-based ISCCP-FD.
2. Besides increasing spatial resolution (from 280 km to 110 km), ISCCP-H has many substantial improvements. For temperature and humidity profiles, new nnHIRS may be better than previous ISCCP-D's TOVS in temporal homogeneity as well as others.
3. New aerosol data MACv2 seems an improvement as validated using 2004 high-quality surface observations.
4. Our cloud-type-dependent statistical VCLC model may be slightly better than previous one for ISCCP-FD; however, because there is no unique solution even with CloudSat-CALIPSO data, it remains to be further improved.
5. The new ISCCP-FH product seems overall slightly better than FD but slightly worse than CERES at surface. The preliminary validation shows that for monthly, regional mean, ISCCP-FH has
   uncertainties $\lesssim$ 10 W/m^2 for TOA and $\lesssim$ 20 W/m^2 for Surface fluxes
6. It may imply a LIMIT we encounter now under the current status of input parameters and, secondarily, radiation modeling. The limit is largely caused by the restriction of the accuracy of the atmospheric, cloud and surface properties, i.e., UNLESS we make substantial improvements on some major input datasets that cause leading errors, substantial reduction on flux calculation uncertainties may not be achievable.

Slide 1: Cover

Slide 2: Earth's Radiation Budget (from global, 2007 mean ISCCP-FH)

This earth-atmosphere budget cartoon is created from the actual global, annual mean ISCCP-FH product for 2007 (after downgrading to 280-km resolution for a fully covered global map of 110-km resolution). It shows that the energy at TOA is perfectly balanced (sum = zero): the incoming SW of 100% for 341.9 W/m^2 is balanced by reflected SW (31%) and OLR (69%), i.e., the earth-atmosphere system neither loses to nor gains energy from outer space in global, 2007 annual mean. The non-reflected SW flux is absorbed partly by the atmosphere and partly by the (land + ocean) surface while all the emitted/reflected LW flux from surface and atmosphere are combined into the 69% of OLR flux with net (= upward minus downward) LW flux of 15% emitted to atmosphere from surface. The atmosphere has various constitutents such as clouds, aerosols, gases, water vapoers that all contrbute to the flux redistribution, including also the surface albedo and temperature for different terrains. Even in this cartoon picture, it shows how complicated the radiation calculation can be.

Slide 3: Why ISCCP FLUX Calculation?

Listed are the seven most important reasons why we need flux datasets such as this ISCCP-FH product as we have explained for the ISCCP-FC anf FD products in the introduction.

Slide 4: Evolution of the ISCCP Flux Products Through Three Generations

Columns 2, 3 and 4 (Left to Right) outline the basic characteristics of the three generations of the ISCCP flux products to illustrate their evolution history: from the earliest ISCCP-FC, to ISCCP-FD and to the current ISCCP-FH with their corresponding three generations of the NASA GISS GCM radaition models (RadII, RadD and RadH), which are what the ISCCP flux products are based on. The ISCCP-FH data are now available for online-access for July 1983 to June 2017 at:

https://isccp.giss.nasa.gov/projects/flux.html

and may become available to the public at NOAA National Centers for Environmental Information (NCEI). The widely used ISCCP-FD product for July 1983 to December 2009 is still available online at the above same site.

Slide 5: Main Radiation-model Improvements of ISCCP-FH

The radiation code for ISCCP-FH production, RadH, is based on the GISS ModelE's radiation code (of 2011), RadE. It has been revised to add several new improvements, of which the most important items are listed here. Among these listed features, adding new values of SW weak line absorption for H2O, O2 and CO2, and update of line absorption for CH4, N2O, etc. has virtually removed the low bias (about 4 – 5 W/m^2 in global average) of atmospheric SW absorption of ModelE as found by Oreopoulos et al. (2012). Thus, it is a significant improvement (see Slide 16 for more specific information). In the meanwhile, the increases of the base atmospheric vertical resolution to a 43-layer standard atmosphere (from original 24 layers) and the treatment for water vapor amount above and below a given layer as well as the water vapor gradient have improved the LW accuracy, especially in the Polar Regions. There are also a few other improvements that will be mentioned later. The RadH code is equivalent to the radiation code of the current NASA GISS ModelE2.1 (Kelley et al., 2020).

Slides 6: Contents of the ISCCP-FH Product

Beginning with ISCCP-FD, the content of the ISCCP flux product was extended from TOA and SRF only (as in ISCCP-FC) to the whole atmospheric flux profile (PRF), TOA and SRF inclusive, as we were able to climatologically construct the cloud vertical structure (CVS) based on a 20-year rawinsonde dataset (Wang et al., 2000; also see slide 11 for ISCCP-FH). Moreover, we have added two more subproducts, MPF and INP, to meet current research needs: there are totally five subproducts, simplified as TOA, SRF, PRF, MPF and INP as shown here. Among them, MPF is more convenient for those users who are only interested in monthly mean values while INP is a virtually complete dataset that can be used to reproduce profile flux products; this is especially useful for in-depth study on cloud-radiation interaction as well as other radiative effects. In addition, beginning with ISCCP-FH, four of the subproducts (excluding INP that remains in binary format) are now available in NetCDF-4 format for even wider access in response to the requests from ISCCP-FD users.

Side 7: Summary of Input Data for ISCCP-FH Production

Here we give a list of all the important input datasets that are used for ISCCP-FH production; all of them reflect the research progress recently achieved since ISCCP-FD was produced. Among them, new atmospheric temperature and humidity profile (nnHIRS) is produced using neural network by NOAA to replace the old TOVS profile for ISCCP-D and ISCCP-FD production, which shows inhomogeneities in the temporal LW flux variations as explained in Zhang et al. (2006). This change does reduce the inhomogeneity. ISCCP-H produces aerosol-corrected surface reflectance based on MACv1 aerosol climatology at 0.65 micron but RadH is based on 0.55 micron and MACv2 so ISCCP-FH has to first remove the aerosol effects on surface reflectance (from ISCCP-H) and then apply the 0.55-micron aerosol effects based on MACv2 to the processed reflectance. In addition, the ISCCP-FH now uses more accurate TSI data that is based on the best SORCE daily solar constant as well as instantaneous earth-sun distance that removes the leap-year errors in ISCCP-FD solar constant that is based on a climatology of 365 days a year.

Side 8: Summary of Output Variables in ISCCP-FH Product

Besides all downwelling and upwelling, SW and LW fluxes at five atmospheric levels for all-, clear- and overcast-sky scenes, the ISCCP-FH product now includes additional surface direct and diffuse downward SW fluxes that are useful for surface validation and other applications (see, e.g., Zhang et al., 2010).

Slide 9: Comparison of main Global, Long-term flux products

As CERES, GEWEX-SRB and ISCCP-FH (and FD) are the principal and most widely used long-term, global flux products, it is necessary to understand their basic similarities and differences as shown here for people to select right one(s) they need to explore.

Slide 10: Improvement by New MACv2 Aerosol Climatology: Example

As mentioned in (3) and (9) of the Slide 7, introducing new MACv2 aerosol data has overall improved our SW flux results. Here we compare surface clear-sky downwelling diffuse and direct flux difference with surface observation ('SRF_OBS') for the original ISCCP-FD ('FD') that uses NASA GISS ModelD's monthly aerosol climatology and revised FD ('MACv2-FD') with aerosol-only change to MACv2 to see how much the improvement could be. The surface observational data are from ten high-quality controlled surface stations that are climate-representative and arranged as from south-most (lowest) to north-most (uppermost): from the South Pole (SPO) to the North Polar Region (FPE) (Zhang et al., 2010). The comparison (differences with SRF_OBS) is for all 2004 monthly means. The left column is for original FD and the right column revised FD; the upper row is for clear-sky diffuse flux ('CDif') and the lower row clear-sky direct flux ('CDir'). Because the NASA GISS ModelE's aerosol input data is not substantially different from ModelD's, this slide may be taken as the

demonstration of the advantage of new MACv2 aerosol data used in ISCCP-FH production. From this slide, we can see substantial improvements for essentially northern hemisphere (all stations above NAU station on Y-axis) but not much change for the southern hemisphere. Note that the total SW downward flux is also improved somewhat (up to 10 W/m^2) but not as much as the separated diffuse and direct fluxes because these two fluxes somewhat compensate each other when they are added up to be total SW flux.

Slide 11: Improvement by New Vertical Cloud Layer Configuration

In developing ISCCP-FD production code, we have introduced a Cloud Vertical Structure (CVS) model to construct climatologically realistic vertical profile clouds so as to calculate realistic flux profile through the entire vertical atmospheric column for the first time on a global scale (Zhang et al., 2004). For ISCCP-FH production, we have improved the vertical cloud profile construction by building up the Vertical Cloud Layer Configuration (VCLC) algorithm. As shown here, it consists of two parts: (1) CVS, essentially the same as the one used for FD but now for 18 original cloud types from ISCCP-H data, and (2) Cloud Layer Thickness Configuration (CLTC) using a combination of previous 20-year rawinsonde climatology and new 5-year CloudSat-CALIPSO climatology. In (1) of this slide, all the 18 original ISCCP-H cloud types are categorized into one of the nine cloud classes, from Ci, Cs, … to St as shown in Column 2, based on cloud top pressure of the 3 ranges of surface – 680, 680 – 440 and 440 – 0 hPa for Low, Middle and High Cloud, denoted as LC, MC and HC, respectively, and cloud optical thickness, τ, with 3 ranges of 0 – 3.6, 3.6 – 23 and 23 – 450 (see Rossow et al., 1996, for ISCCP-D, but whose largest τ is 379 instead of the current 450 for ISCCP-H). There may be some Sub-cloud classes, Thin and Thick (Column 3), based on τ values subdivided at $\tau = 1.3$ for low τ of 0 – 3.6 and at $\tau = 9.4$ for middle τ of 3.6 – 23, for MC and HC classes, respectively, if necessary. Column 4 shows such cloud-class-based, eight CVS types, e.g., 1H for one high cloud layer, HML for three separated High, Middle and Low cloud layers and 1 H-M-L for one cloud layer from high through middle to low pressure layer. The original total column τ will be redistributed, proportional to the sum of the new cloud layers' thickness if there are two or more cloud layers for a determined CVS type. The total column τ is conserved except for the two special CVS types, HM* and HL*, for which we have to redistribute the original 1-layer-based τ to new two-cloud-layer based, consistent with assumed satellite detection. The cloud top position of all the cloud layers for a determined CVS type is based on either current cloud top temperature (if available) or climatological cloud information from ISCCP-H. In (2), the cloud thickness (therefore cloud base) is now a function of cloud optical thickness τ, longitude, latitude, ocean/land, and month, where τ and longitude are new variables that ISCCP- FD did not use because of lack of cloud profile data (like CloudSat-CALIPSO) at that time. By these steps, we are able to construct a vertical profile of clouds with all cloud layers interleaved with possible clear-air layers for a determined CVS, for which cloud phase and particle size are also determined based on all available information from ISCCP-H and climatology before calculating the flux profile.

Slide 12: Improvement by new VCLC: Example -- Vertical Cloud Fraction Profile: 0707 Ocean & Land

Here is an example of monthly-mean vertical profile of cloud amounts for ocean (left) and land (right), respectively, for July 2007, to see how the new VCLC algorithm performs versus the old one. The slide compares the monthly vertical profiles of cloud fraction (in %) for the CloudSAT-CALIPSO, the original FD, the revised FD using new VCLC, and new FH (also using new VCLC), respectively with their symbols shown in the legend box. The pressure level is arranged such that the Y-axis is from the ground surface (1000 hPa) to TOA (~0 hPa). Compared with CloudSat-CALIPSO (black solid line), overall both the revised FD (blue upward empty triangle) and FH (brown empty diamond with dashed line) outperform the original FD's cloud profile (red solid circle), especially for middle clouds and, in addition, FH has better high cloud profile than the revised FD showing the improvement in high-cloud detection in ISCCP-H product. The CALIPSO lidar has much higher sensitivity to detect high clouds, thus CloudSat-CALIIPSO's high cloud amount is higher than FH's, but those high clouds (mainly thin cirrus, see Rossow and Zhang, 2010) may have very low τ value that may not affect the flux much. For low clouds CloudSAT-CALIPSO may have some difficulty to determine an

accurate low cloud profile because of attenuation, so its uncertainty is larger. Given all of these issues for both ISCCP and CLoudSat-CALIPSO datasets, the current VCLC is in need of further improvement.

Slide 13: Preliminary validation against CERES for 2017 Monthly means: All-sky at TOA

As preliminary validation, we use all 2017 monthly means to compare the ISCCP-FH, ISCCP-FD with the Clouds and the Earth's Radiant Energy System (CERES) and the Baseline Surface Radiation Network (BSRN) for TOA and surface validation, respectively. We also compare with CERES and in-atmosphere for ensemble-based validation (Zhang et al., 2006) since CERES is also a flux product for atmospheric fluxes. This slide shows the comparison for all-sky net ('net') fluxes, cloud effects ('ce') and albedo at TOA, where, Stdv, cor coef, intercept, Nrm dev and Eq cell # stand for standard deviation, correlation coefficient, intercept, normal standard deviation calculated based on the distance of a reference dataset (here FH or FD) to their regression line (with CERES) that is a measure of rms scattering for the reference dataset, and total equal-area cell number of all available 2017 monthly means (if it is different in original spatial resolution, a higher-resolution equal area map is downgraded to the same as a low-resolution dataset). From the table, we can see that FH is better than FD by a fraction of a percent for all bias ('mean difference'), standard deviation (Stdv) and Nrm dev for albedo while only slightly better for SW_net. For SW_ce, although FH has ~3 W/m^2 lower bias than FD, its variation is worse than FD by ~2 W/m^2. For LW fluxes, FH is actually worse than FD by up to ~4 W/m^2 in LW_net bias (but FH's LW_net has slightly smaller Stdv and Nrm dev than FD). Note that FH is now has the same higher spatial resolution of 110 km as CERES while FD has 280 km resolution so its comparison with CERES is for downgraded 280-km resolution that usually would result in better agreement through the average for CERES

Slide 14: Preliminary validation against CERES for 2017 Monthly means: Clear-sky at TOA

For clear-sky fluxes at TOA, FH seems slightly worse than FD by about half percent and ~2 W/m^2 for albedo and SW_net, respectively. For LW_net, FH is nearly ~4 W/m2 worse than FD in bias, but again its Stdv and Nrm dev are slightly better than FD. Note, however, that the meaning of 'clear sky scene' is different between CERES and the calculated global clear-sky scene which is the same as all-sky scene except that all cloud τ is set to zero in clear-sky calculation, i.e., there are environmental differences between the two clear-sky concepts.

Slide 15: Preliminary validation against CERES for 2017 Monthly means: In-atmosphere all-sky

For all-sky SW fluxes in the atmosphere, FH is closer (than FD) to CERES by up to ~5 W/m^2 (in SW_net bias) except Stdv and Nrm dev of SW_ce for which FD has better agreement with CERES. For LW_net, FD is closer to CERES by 3.5 W/m^2 in bias but FH has smaller Stdv and Nrm dev than FD; for LW_ce. FH has smaller bias with CERES than FD but FD has smaller Stdv and Nrm dev. The fact that the FH's SW_net is ~5 W/m^2 closer to CERES than FD demonstrates much improved SW's atmospheric absorption in RadH code as mentioned above.

Slide 16: Preliminary validation against CERES for 2017 Monthly: In-atmosphere clear-sky

For atmospheric clear-sky fluxes, FH has a better agreement with CERES than FD, especially substantially improvement for SW_net by 5.6 W/m^2 as a demonstration of improved atmospheric absorption of RadH code.

Slide 17: BSRN Stations used for Surface-flux Validation (39 are data-available for 2007)

We now compare all the monthly mean surface fluxes from CERES, FD and FH for 2007 with the ground-based measurements, the observed data from BSRN. Here is the list of the 39 BSRN stations, whose 2007 data is used for surface validation here; the ten red-colored stations are what were used in Slide 10 for demonstrating the effects of aerosol data change from NASA GISS' climatology to MACv2.

Slide 18: Preliminary validation against BSRN: for 2017 Monthly Mean

With BSRN as ground 'truth', overall CERES seem to have the best performance, though ISCCP-FH outperforms CERES by 3 W/m^2 for SWdn in bias and 5 W/m^2 for LWup in bias. ISCCP-FD has the worst performance. ISCCP-FH is overall improved over ISCCP-FD: by up to ~13 W/m^2 for SWup bias while by ~2-3 W/m^2 for SWdn and LWdn bias, Stdv and Nrm dev.

Slide 19: Preliminary Uncertainty Estimate for monthly/regional ISCCP-FH

We summarize the above validation results. Overall ISCCP-FH is slightly better than FD but their uncertainties are virtually about the same.

Slide 20: Conclusions

Based on the above presentation, we make several concluding remarks as stated here. We mention 'limit' based on the current error estimates for all the input variables of the atmospheric and surface physical properties, which we think are unlikely to have substantial improvement in near future. Accordingly, the current flux uncertainty may not change much in a short time.